


Sequence and structure requirements for specific recognition of HIV-1 TAR and DIS RNA by the HIV-1 Vif protein

S  verine Freisz, Joelle Mezher, Lamine Hafirassou, Philippe Wolff, Yves Nomin  , Christophe Romier, Philippe Dumas & Eric Ennifar


To cite this article: S  verine Freisz, Joelle Mezher, Lamine Hafirassou, Philippe Wolff, Yves Nomin  , Christophe Romier, Philippe Dumas & Eric Ennifar (2012) Sequence and structure requirements for specific recognition of HIV-1 TAR and DIS RNA by the HIV-1 Vif protein, RNA Biology, 9:7, 966-977, DOI: [10.4161/rna.20483](https://doi.org/10.4161/rna.20483)

To link to this article: <http://dx.doi.org/10.4161/rna.20483>



 View supplementary material 

 Published online: 01 Jul 2012.

 Submit your article to this journal 

 Article views: 120

 View related articles 

 Citing articles: 4 View citing articles 

Sequence and structure requirements for specific recognition of HIV-1 TAR and DIS RNA by the HIV-1 Vif protein

S  verine Freisz,¹ Joelle Mezher,¹ Lamine Hafirassou,¹ Philippe Wolff,¹ Yves Nomin  ,² Christophe Romier,³ Philippe Dumas¹ and Eric Ennifar^{1,*}

¹Architecture et R  activit   des ARN; CNRS/Universit   de Strasbourg; Institut de Biologie Mol  culaire et Cellulaire; Strasbourg, France; ²Equipe Oncoprot  ines; Institut de Recherche de l'  cole de Biotechnologie de Strasbourg; Universit   de Strasbourg; Illkirch, France; ³D  partement de Biologie et G  nomique Structurales; IGBMC, CNRS/INSERM Universit   de Strasbourg; Illkirch, France

Keywords: HIV, biophysics, RNA-protein interactions, microcalorimetry

The HIV-1 Vif protein plays an essential role in the regulation of the infectivity of HIV-1 virion and in vivo pathogenesis. Vif neutralizes the human DNA-editing enzyme APOBEC3 protein, an antiretroviral cellular factor from the innate immune system, allowing the virus to escape the host defense system. It was shown that Vif is packaged into viral particles through specific interactions with the viral genomic RNA. Conserved and structured sequences from the 5'-noncoding region, such as the Tat-responsive element (TAR) or the genomic RNA dimerization initiation site (DIS), are primary binding sites for Vif. In the present study we used isothermal titration calorimetry to investigate sequence and structure determinants important for Vif binding to short viral RNA corresponding to TAR and DIS stem-loops. We showed that Vif specifically binds TAR and DIS in the low nanomolar range. In addition, Vif primarily binds the TAR UCU bulge, but not the apical loop. Determinants for Vif binding to the DIS loop-loop complex are likely more complex and involve the self-complementary loop together with the upper part of the stem. These results suggest that Tat-TAR inhibitors or DIS small molecule binders might be also effective to disturb Vif-TAR and Vif-DIS binding in order to reduce Vif packaging into virions.

Introduction

The HIV-1 Virion Infectivity Factor (Vif) is a small basic protein of 192 amino acids (23 KDa, pI = 10.7). It has been known for a long time to be essential for viral replication in some, but not all, cell lines.¹⁻⁵ In absence of Vif, human antiviral proteins from the APOBEC3 cytidine deaminase family are packaged into virions and exhibit anti-HIV-1 activity mostly by two mechanisms: (1) deamination of cytidines in the minus strand of the proviral DNA,⁶⁻⁸ and (2) inhibition of the reverse transcription through a deaminase-independent mechanism.⁹⁻¹¹ APOBEC3G, formerly known as CEM15, was first identified as a potent endogenous inhibitor for replication of several retroviruses, including HIV-1.^{8,12,13} Later on, other members of the APOBEC3 family have been identified as HIV-1 restriction factors: APOBEC3F,^{12,14,15} APOBEC3B,^{12,16} APOBEC3DE¹⁷ and APOBEC3H.¹⁸ The anti-retroviral activity of APOBEC3DE¹⁹ and APOBEC3H^{17,20} is however still controversial and, with the exception of APOBEC3F, these proteins are poorly expressed in human lymphoid tissues and only lead to a moderate effect on HIV-1 infection.

To bypass the host defense system and counteract APOBEC3 action, Vif dramatically reduces APOBEC3G incorporation into the virion using several pathways (for a review on

Vif-APOBEC3 interactions see refs. 21-23). First, Vif interacts with APOBEC3F/G and hijacks the human E3 ubiquitin ligase complex consisting of Cullin5, ElonginB, ElonginC and a zinc RING finger protein (Rbx), leading to a polyubiquitination of APOBEC3F/G and to its degradation by the 26 S proteasome.²⁴⁻²⁸ It was recently shown that, in addition to the E3 ubiquitin ligase complex, the transcription cofactor CBF-   is also recruited by Vif and is required for the APOBEC3G degradation.²⁹⁻³¹ Interestingly, APOBEC3B¹⁶ and APOBEC3H¹⁸ have been reported to escape this Vif-mediated degradation. Besides APOBEC3 degradation, Vif negatively regulates APOBEC3G transcription through binding to 5'-UTR of APOBEC3G mRNA.^{28,32,33} Finally, Vif also reduces APOBEC3G packaging into the virion by competing for the same Gag and viral RNA binding sites, thus leading to a physical exclusion of APOBEC3G from the budding virion.^{27,32,34,35} It was indeed shown by several studies that Vif is an RNA-binding protein that specifically recognizes the viral RNA in vitro and in infected cells.³⁶⁻³⁹

Several conserved domains have been identified in Vif:⁴⁰ (1) a tryptophan-rich N-terminal domain responsible for RNA and APOBEC3 binding, (2) a HCCH motif that coordinates a Zn²⁺ ion and which is responsible for the binding with Cullin5, (3) an ¹⁴⁴SLQ(Y/F)LA¹⁴⁹ motif, named "SOCS-box", responsible

*Correspondence to: Eric Ennifar; Email: e.ennifar@ibmc.u-strasbg.fr
Submitted: 03/20/12; Revised: 04/18/12; Accepted: 04/23/12
<http://dx.doi.org/10.4161/rna.20483>

for the interaction with Elongin B/C, (4) a proline-rich region containing a ¹⁶¹PPLP¹⁶⁴ motif involved into Vif multimerization and (5) a C-terminal domain interacting with Gag and the cellular membrane (Fig. 1A).

Using RNase-T1 footprinting, an enzyme that cleaves after a guanine residue accessible to solvent, preferential Vif RNA binding sites have been mapped in the 5'-region of the genomic RNA.^{37,41} The strongest affinity was observed for the apical part of the TAR stem-loop, the poly(A) stem and a short region in *gag*, whereas the primer-binding site (PBS), the SL1 and SL2 stem-loops, as well as a purine-rich single-stranded region adjacent to the Gag start codon have been identified as lower-affinity Vif-binding sites.³⁷ Binding to the upper part of the TAR stem-loop was subsequently confirmed on short RNA fragments using steady-state fluorescence spectroscopy.^{41,42}

In the present work, we used Isothermal Titration Calorimetry (ITC) to study the binding thermodynamics of Vif binding to the HIV-1 genomic RNA TAR and Dimerization Initiation Site (DIS) stem-loops (Fig. 1B). Using various mutants of TAR and DIS mutants (Fig. 1C), we could define the sequence and structure requirements for the Vif specific binding to these regions of the viral RNA. Our results show that Vif specifically and tightly binds both TAR and DIS sequences in the low nanomolar range. Vif primarily binds the UCU lateral bulge of the TAR, and secondarily the apical loop. Regarding binding to the DIS loop-loop complex, we found that mutations of the DIS loop preventing DIS dimerization also affect Vif binding, whereas the purine-rich internal loop of the DIS stem is clearly dispensable. Our data also indicate that the upper part of the DIS stem might be important for protein binding. Taken together, these results open the perspective of developing drugs that would prevent Vif binding to the TAR and DIS stem-loops and, consequently, reduce Vif packaging. They also suggest that Vif might compete with APOBEC3G for binding the DIS stem-loop, leading to an exclusion of the restriction factor from the viral particle.

Results

Biophysical characterization of the full-length HIV-1 Vif protein. It has been shown that Vif monomers self-associate into multimers both in vitro and in infected cells.^{43,44} The ¹⁶¹PPLP¹⁶⁴ motif is important for this Vif oligomerization, for viral infectivity,^{42,45–47} and was also reported to interact with Elongin B.⁴⁸ Mutation of the PPLP motif into AALA reduces, but does not abolish, oligomerization.⁴² This strong tendency of Vif to self-associate and aggregate^{33,42,49,50} has also thwarted attempts to obtain large quantities of high-quality and homogenous protein. Here, we successfully expressed and purified milligrams of recombinant full-length wild-type Vif, typically about 13 mg of purified protein per liter of cell culture, thus allowing detailed ITC analysis of Vif/RNA interaction. Because the recombinant protein was always found insoluble when expressed in *E. coli*,^{33,41,42,49–51} Vif was solubilized using guanidine hydrochloride and subsequently refolded by dialysis. The proper folding of the protein was assessed using far-UV circular dichroism (CD). Secondary structure calculations from the CD spectra

yielded 20% α -helix, 26% β -strands, 23% turns and 30% of disordered structure (which was expected in the Gag/Membrane and Elongin B/C binding domains in absence of their partners), with good agreement between calculated and experimental data (Fig. 2A). This result shows that the produced protein is correctly folded after denaturation/renaturation and observed secondary structure is approximately in agreement with recently published Vif CD data.^{42,49,52} However, a significant increase in α -helix and decrease in β -strands contents is noticeable compared with previous reports (Table 1). This difference might be responsible for the increased solubility of our Vif sample, in line with a previous study showing that formation of β -sheets might be responsible for Vif aggregates.⁵³

We next analyzed the homogeneity of Vif using Dynamic Light Scattering (DLS) to ensure that our sample was monodisperse and free of aggregates, two necessary conditions required for reliable and good quality ITC analysis. Based on DLS measurements performed at various protein concentrations (4 to 200 μ M), we found that the protein sample was highly monodisperse with a polydispersity index of 16.3% and a hydrodynamic radius of 7 nm (Fig. 2B). This is in good agreement with the recent report of Bernacchi et al.⁴² but quite different from Gallerano et al. who obtained a hydrodynamic radius of 24 nm with a polydispersity index of 51%. Our DLS measurements performed at 10%, 5% and 2.5% glycerol concentrations did not show any significant variations down to 2.5% of glycerol, whereas massive aggregation was observed in absence of glycerol (not shown). To investigate the oligomerization state of our Vif construct, the average molecular weight of the sample was evaluated using Static Light Scattering (SLS). In a buffer containing 5% glycerol, we observed an average molecular weight of 270 kDa, which corresponds to multimers containing 10 to 11 Vif proteins and is in agreement with a recent similar study based on both size exclusion chromatography and DLS.⁴² We concluded from these experiments that, even in absence of the co-factor CBF- β , the produced wild-type Vif protein can be obtained under a soluble, homogenous and stable form at concentrations up to 400 μ M, and is therefore suitable for ITC measurements.

Vif binding to HIV-1 TAR RNA stem-loop. In a further step, isothermal titration calorimetry (ITC) was used to characterize Vif binding to the TAR stem-loop. ITC is a true in-solution technique and is considered the “gold standard” assay for binding since it directly provides, in one single experiment, the complete binding profile between two molecules, without any labeling requirement (reviewed in ref. 54–56). Typically, the ligand solution is repetitively injected in small aliquots from an automatic syringe into a thermally isolated stirred cell containing the protein. In an ITC experiment, one physically measures the heat generated or absorbed during a binding reaction. A direct measurement of the binding thermodynamics allows determination of the binding affinity (K_a), enthalpy and entropy changes (ΔH and ΔS) and stoichiometry (N) between two molecules.

Several Vif aliquots (1.5 to 2.0 μ l at a \sim 200 μ M concentration) were injected into 15 μ M TAR RNA. This protocol was used since the reverse titration (injections of concentrated TAR aliquots into diluted Vif protein) systematically led to aggregation

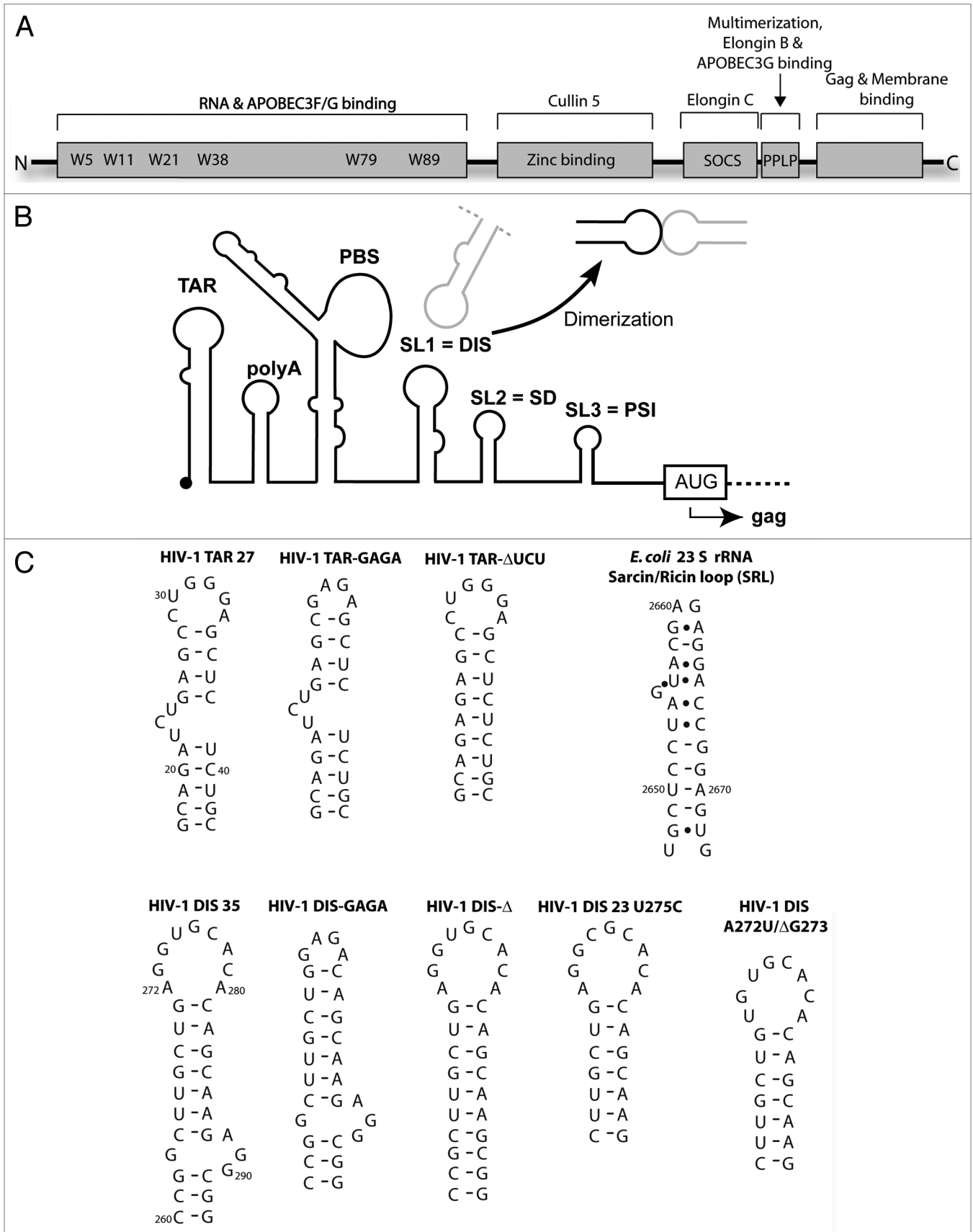


Figure 1. (A) Schematic representation of identified Vif functional regions. (B) Secondary structure of the 5'-untranslated region of the HIV-1 RNA genome. (C) RNA sequences used in this study.

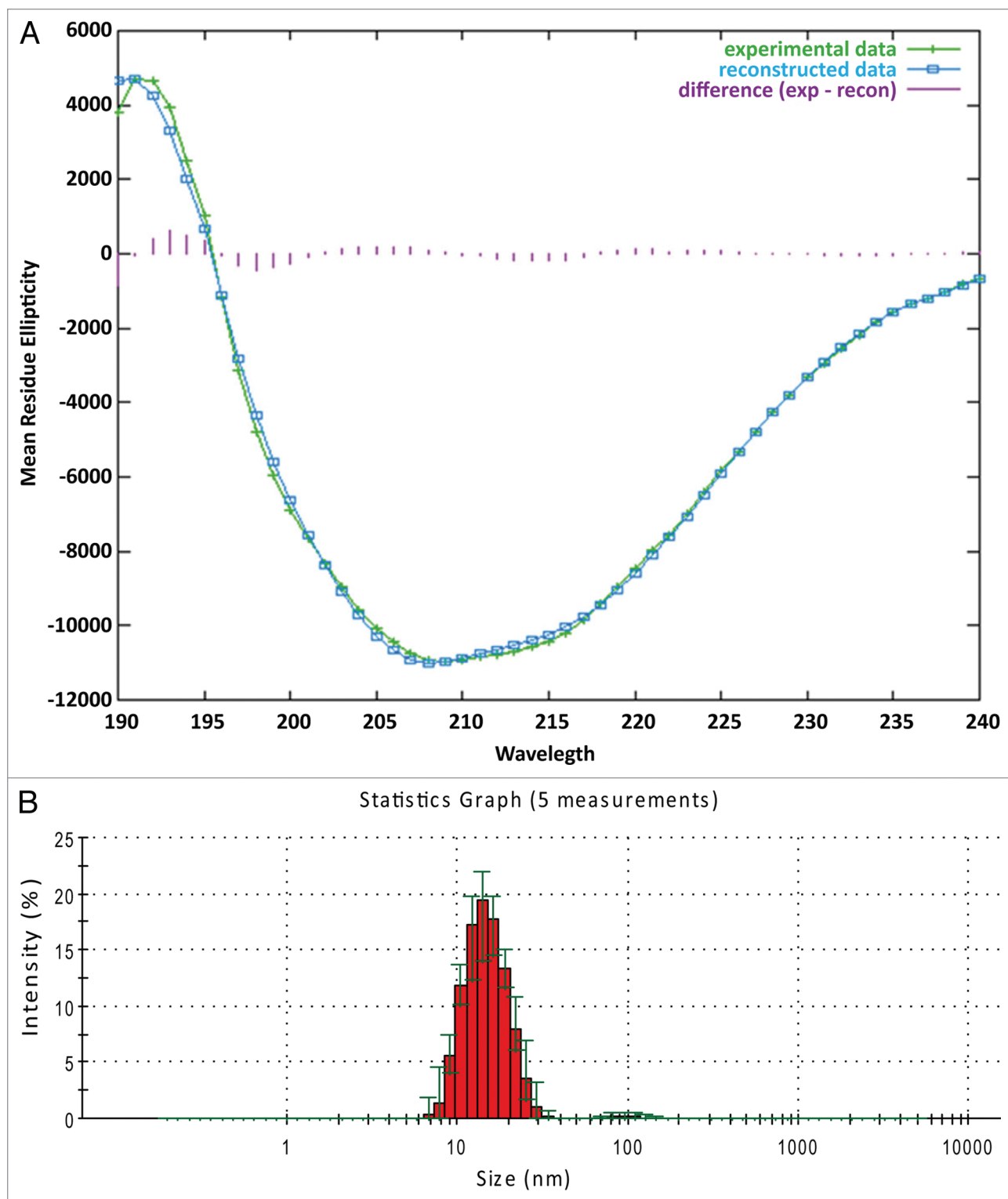


Figure 2. Biophysical characterization of purified Vif protein. (A) Far-UV spectra of the Vif protein and reconstructed data. (B) Dynamic light scattering profiles of the HIV-1 Vif showing a mean diameter of 14 nm.

of the protein/RNA complex in the ITC cell as judged by an abnormally high exothermic signal and baseline drift. In addition, most of our data were acquired at 30°C since baselines were more stable at this temperature. Some data were nevertheless

obtained at 25°C, providing access to a temperature dependence of the binding enthalpy (see **Sup. data**). In our experimental conditions and in presence of 200 mM KCl, we observed a specific Vif binding to the TAR27 RNA (**Figs. 1C and 3**). The

observed dissociation constant ($K_d \sim 160$ nM) is associated with a rather large negative enthalpy variation ($\Delta H = -10.6$ kcal/mol, corresponding to an exothermic process) and a slightly negative entropy variation (Fig. 3 and Table 2). The specificity of the protein/RNA binding is assessed by the 1:1 observed stoichiometry. This implies either that each Vif protein within a multimer is able to bind independently one TAR RNA, or that Vif multimers dissociate upon TAR binding. In a previous report it was found that, upon Vif binding to short RNA constructs, the mean hydrodynamic radius of resulting Vif/RNA complexes significantly increased compared with the free protein.⁴² This observation therefore suggests that RNA binding does not promote Vif multimer dissociation. An increase of monovalent salt concentration to 300 mM, in order to reduce potential unspecific electrostatic Vif/RNA interactions, only led to a moderate decrease of the dissociation constant (1.8-fold). This suggests a significant contribution of hydrophobic interactions in the Vif/TAR interaction, likely through the tryptophan-rich RNA binding region (Trp5, Trp11, Trp21, Trp38, Trp79 and Trp89).

To further confirm the specificity of the Vif/TAR interaction, we used the *E. coli* 23 S RNA sarcin-ricin loop (SRL), a highly structured RNA stem-loop similar in size, but unrelated to TAR (Fig. 1C), as a control for unspecific RNA binding. Mixing of Vif into SRL RNA only led to a weak endothermic signal ($\Delta H = -5.0$ kcal/mol), that could not be fitted using a single site binding model (Fig. 4 and left). Furthermore, increasing the salt concentration to 300 mM led to a complete loss of interaction (Fig. 4 and right).

In order to define structure and sequence determinants for Vif binding to TAR RNA, we next used two TAR mutants (Fig. 1C): TAR-GAGA, where the wild-type five nucleotide apical loop was replaced by a GAGA tetraloop (a member of thermostable GNRA tetraloops), and TAR- Δ UCU, where the apical three nucleotide lateral bulge was deleted (Fig. 1C). ITC data obtained on the TAR-GAGA (in 200 mM KCl) mutant did not reveal any significant change in Vif binding. The observed stoichiometry ($n = 0.7$) was still close to 1.0 and both the dissociation constant (1.2-fold decrease) and the enthalpy variation ($\Delta H = -8.9$ kcal/mol) were only moderately affected (Fig. 3 and Table 2). Notably, the small decrease in the enthalpic component is compensated by a slightly positive entropic term. Likewise, the protein binding to this mutant TAR sequence was only poorly affected in a buffer containing 300 mM KCl: the affinity decreased ~ 2 -fold compared with binding to the TAR27 in the same conditions, together with a slight decrease of ΔH (Fig. 3 and Table 2).

On the contrary to the mutation of the apical loop, deletion of the UCU lateral bulge severely affected Vif binding as revealed by ITC data obtained with the TAR- Δ UCU sequence. In conditions with 200 mM KCl, the stoichiometry significantly increases to $n = 2.0$ and the K_d decreased to about 1 μ M, which represents a 6.7-fold loss compared with wild-type sequence. In a buffer with 300 mM KCl, no Vif binding could be detected anymore (Fig. 3 and Table 2). We conclude from this set of experiments that Vif likely binds primarily the UCU lateral bulge of TAR through specific hydrophobic interactions. This interaction might be

Table 1. Comparison of Vif secondary structure composition derived from CD data

Reference	α -helix	β -strands	turns	disordered
33	6.5%	41.5%	12%	40%
49	11%	33%	28%	28%
52	6%	32%		62%
This work	20%	26%	23%	30%

Our data and those from references 33 and 49 were obtained using the same CDSSTR algorithm and reference set database, thus ruling out any influence of the data processing.

reinforced by subsequent (mostly electrostatic) interactions with the TAR apical loop.

Vif binding to HIV-1 DIS RNA kissing-loop. We next investigated the Vif binding to the DIS stem-loop. Because of the self-complementarity in the loop, the wild-type 35-mer DIS monomer forms DIS loop-loop dimers (also called kissing-loop) in native conditions (reviewed in refs. 57 and 58). Alternatively, an extended duplex dimeric form can also be obtained in vitro depending on RNA folding conditions. In this study, care was taken to use folding conditions leading essentially to DIS loop-loop complexes (see materiel and methods). To define RNA determinants for the protein binding, two mutants were designed (Fig. 1C): (1) the DIS- Δ mutant, where the internal purine-rich loop was deleted. It was shown that this internal loop is important for viral infectivity⁵⁹ and might be involved into binding of the NCp7 nucleocapsid protein;⁶⁰ (2) the DIS-GAGA mutant containing a GAGA tetraloop instead of the nine nucleotide apical loop. As a consequence for this mutation, the DIS-GAGA mutant was not able to form dimers in vitro in our conditions as evaluated by native polyacrylamide gels (not shown).

ITC data performed in presence of 200 mM KCl on the wild-type DIS 35-mer showed that Vif specifically and tightly ($K_d = 63$ nM) binds the DIS loop-loop complex with a 1:1 stoichiometry (one Vif binding per DIS stem-loop monomer, Fig. 5 and Table 2). As seen previously for TAR binding, the Vif/DIS interaction is exothermic and mostly driven by enthalpic contributions ($\Delta H = -9.1$ kcal/mol, $-T\Delta S = -0.9$ kcal/mol). An increase of the monovalent salt concentration to 300 mM KCl led to a 2.8-fold loss in affinity ($K_d = 177$ nM) but still preserved the specificity of the interaction ($n = 0.8$). Deletion of the purine-rich internal loop of the DIS (sequence DIS- Δ , Fig. 1C) does not significantly affects Vif binding, neither in 200 mM KCl, nor in 300 mM KCl. The affinity of Vif for this DIS mutant only drops about 1.2-fold compared with the wild-type DIS and the stoichiometry remains close to 1:1 (Fig. 5 and Table 2). As seen previously for the TAR-GAGA mutant, a loss in the negative binding enthalpy is compensated by a positive entropic contribution for this DIS- Δ sequence. Experiments performed on the DIS-GAGA sequence revealed more significant differences in Vif binding. In conditions based on 200 mM KCl, a 2-fold loss in affinity was observed. In higher salt concentration, it was not possible to properly fit ITC corrected injection heats using a single site binding model used for all other ITC data (Fig. 5), suggesting a more complex protein binding.

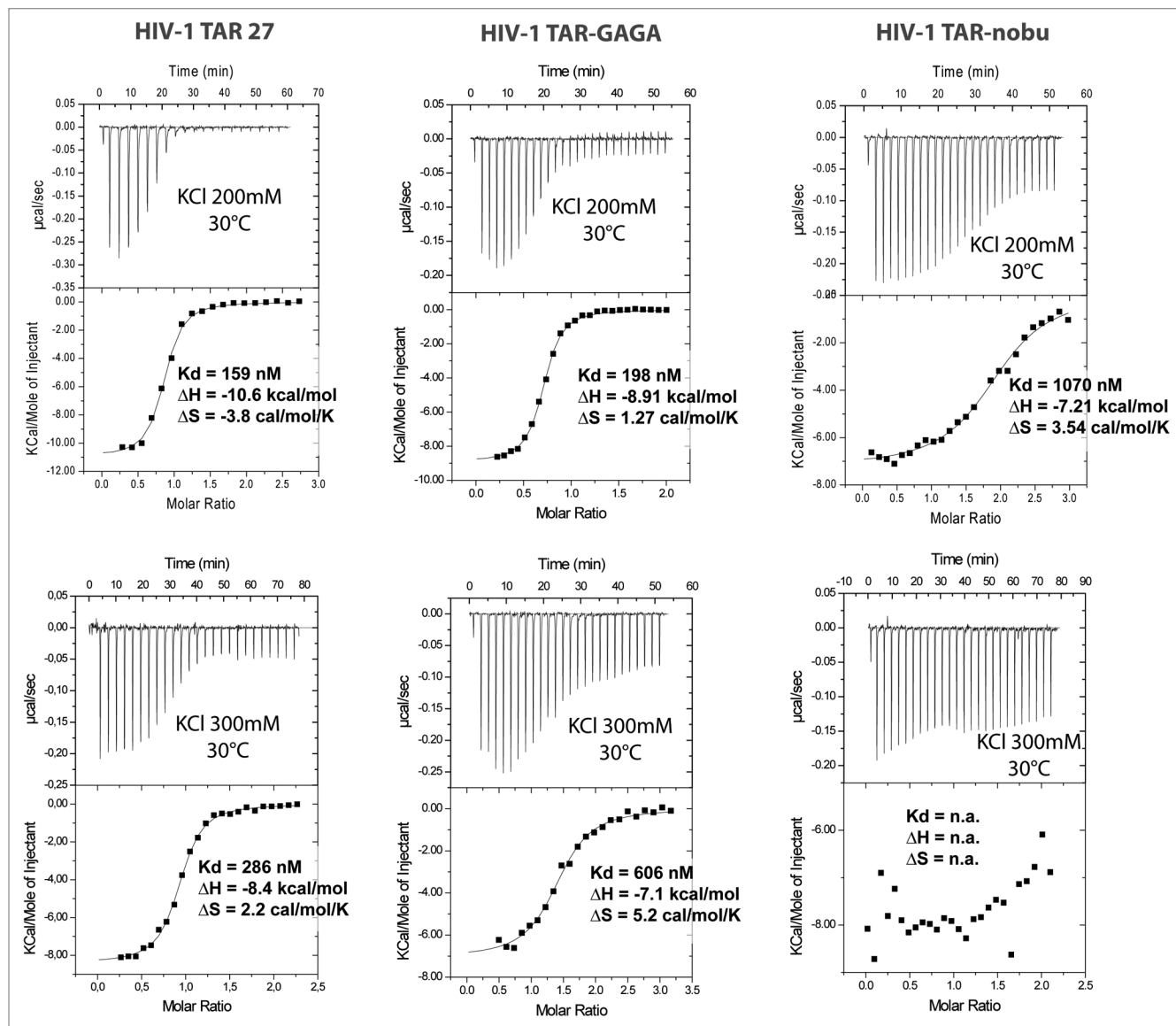


Figure 3. ITC profiles for the titration of HIV-1 Vif on the HIV-1 TAR27 stem-loop and mutant TAR sequences at 30°C and in presence of 200 or 300 mM of KCl. Each heat burst curve is the result of a 1.5 or 2.0 µl injection of 200 µM Vif in a 15 µM RNA solution. The corrected injection heats were derived by integration of the ITC profiles and were fitted with a one site binding model. "n.a." denotes "not applicable" since no binding was observed.

Table 2. Summary of binding parameters derived from ITC measurements for Vif binding to HIV-1 TAR and DIS wild-type and mutant sequences

200 mM KCl 300 mM KCl	DIS-WT		DIS-Δ		DIS-GAGA		TAR-WT		TAR-GAGA		TAR-ΔUCU	
N	1.1	0.8	1.0	0.7	1.1	n.d.	0.8	0.9	0.7	1.4	2.0	n.d.
ΔH (kcal/mol)	-9.1 ± 0.1	7.1 ± 0.1	-8.0 ± 0.1	-5.9 ± 0.1	-7.1 ± 0.1	n.d.	-10.6 ± 0.2	-8.4 ± 0.1	-8.9 ± 0.1	-7.1 ± 0.2	-7.2 ± 0.2	n.d.
ΔS (cal/mol/deg)	2.9	7.4	6.3	11.0	8.3	n.d.	-3.8	2.2	1.3	5.2	3.5	n.d.
K _d (nM)	63 ± 3	177 ± 21	75 ± 9	229 ± 16	121 ± 10	n.d.	159 ± 20	286 ± 22	198 ± 13	606 ± 81	1070 ± 122	n.d.

N.d. denotes "not determinable" since accurate values could not be obtained.

In order to understand the role of the DIS loop dimerization in Vif binding, we tested the protein interaction on a DIS loop mutant with a U275C mutation that prevents self-dimerization (sequence DIS 23 U275C, Fig. 1C). In addition, this mutant is deprived of the lower part of the DIS stem, including the purine-rich internal loop that is dispensable for Vif binding as shown previously. In conditions with 200 mM KCl, the obtained ITC binding profile is quite similar to the one observed with the DIS-GAGA mutant: a slight increase in the stoichiometry ($n = 1.2$) together with a ~ 2 -fold drop of the affinity constant (Fig. S1 and top). In presence of 300 mM KCl, the affinity decreased to $1.3 \mu\text{M}$, highlighting the role of electrostatic interactions in the Vif/DIS U275C interaction. We also noticed that ITC data collected with this DIS mutant were rather noisy (Fig. S1 and top), which might suggest some aggregation of protein/RNA complexes. Finally, to evaluate a possible binding of Vif to the DIS stem, we used a DIS A272U/ Δ G273 mutant (Fig. 1C). Because of the perfect complementarity of the eight-nucleotide loop, this sequence forms a 22 base-pairs duplex in vitro instead of a loop-loop complex (Fig. S1). In a buffer containing 200 mM KCl, Vif binds rather tightly to this sequence since we observed only a ~ 2 -fold loss in affinity compared with wild-type DIS, however with a substantial increase in the stoichiometry ($n = 1.6$). As observed previously for the DIS U275C mutant, the Vif affinity for the DIS A272U/ Δ G273 mutant was severely affected in presence of 300 mM KCl ($K_d = 0.7 \mu\text{M}$).

It thus appears that Vif behaves quite similarly with DIS A272U/ Δ G273 and DIS U275C, i.e., in DIS sequences where the 7-base-pair upper part of the stem is preserved. A detailed look in the binding thermodynamics of the Vif-DIS A272U/ Δ G273 and Vif-DIS U275C interactions in 200 mM KCl (Fig. S1) reveals an important loss in the binding enthalpy ($\Delta H = -5.0$ and -4.3 kcal/mol, respectively) compensated by an important gain in binding entropy ($\Delta S = 15.4$ and 17.1 cal/mol/K, respectively) compared with binding to the wild-type DIS kissing-loop complex. This suggests that Vif binds the wild-type DIS and mutant sequences using slightly different binding mechanisms, likely mixed hydrophobic and electrostatic interactions on the wild-type DIS, but mostly electrostatic interactions in DIS loop mutants since binding is more sensitive to monovalent salt concentration.

We therefore conclude from this series of Vif/DIS experiments that Vif interacts both with the DIS loop-loop helix and the 7-base-pair stem adjacent to the loop, but not with the purine-rich internal loop. An increase in salt concentration only moderately affects Vif binding to the DIS wild-type and DIS- Δ sequences, but more severely the binding to DIS-GAGA, DIS UC275 and DIS A272U/ Δ G273 mutants, i.e., all sequences

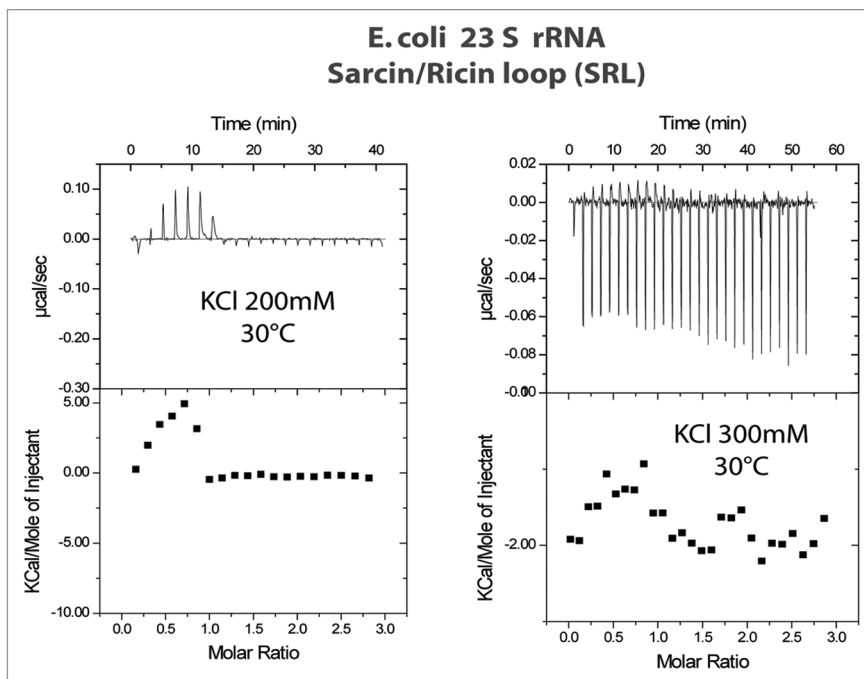


Figure 4. ITC profiles for the titration of HIV-1 Vif on the *E. coli* 23 S rRNA Sarcin/Ricin Loop at 30°C and in presence of 200 or 300 mM of KCl. Each heat burst curve is the result of a 1.5 or 2.0 μl injection of 200 μM Vif in a 15 μM RNA solution. Data could not be fitted using binding models available in the Origin ITC software and are likely relevant of unspecific Vif/RNA binding.

affecting the loop-loop complex integrity but preserving the 7-base-pair stem (Fig. 5 and Table 2). As a consequence, Vif likely binds the DIS kissing-loop mostly through hydrophobic interactions and the 7-base-pair stem through electrostatic interactions. Because A272 and G273 are observed in an extrahelical conformation in crystal structures of the DIS kissing-loop complex,^{61,62} we can hypothesize that they are involved into stacking interactions with some Vif tryptophan residues. Furthermore, because of structural similarities between the DIS kissing-loop complex and DIS extended duplex forms,^{63,64} which is putatively present in mature virions and obtained after isomerization by the NCp7 protein,^{65,66} we can anticipate that Vif should also specifically interact with this form of the DIS dimer.

Discussion

Here we show using Isothermal Titration Calorimetry that Vif specifically binds HIV-1 TAR stem-loop and DIS kissing-loop complex. Using a set of TAR and DIS mutants, we elucidated RNA determinants of Vif interaction to both sequences.

We found that Vif primarily recognizes the TAR UCU lateral bulge, which appears to be essential for the protein binding. The TAR apical loop might play a secondary role in the Vif binding since it contributes positively, but moderately, to the interaction. Interestingly, it is well-established that the TAR UCU lateral bulge is recognized by an arginine-rich RNA-binding motif of the HIV-1 Tat protein,^{67,68} another small regulatory basic protein. This Tat/TAR interaction is essential for Tat-dependent transcriptional activation.⁶⁹ Several low molecular-weight

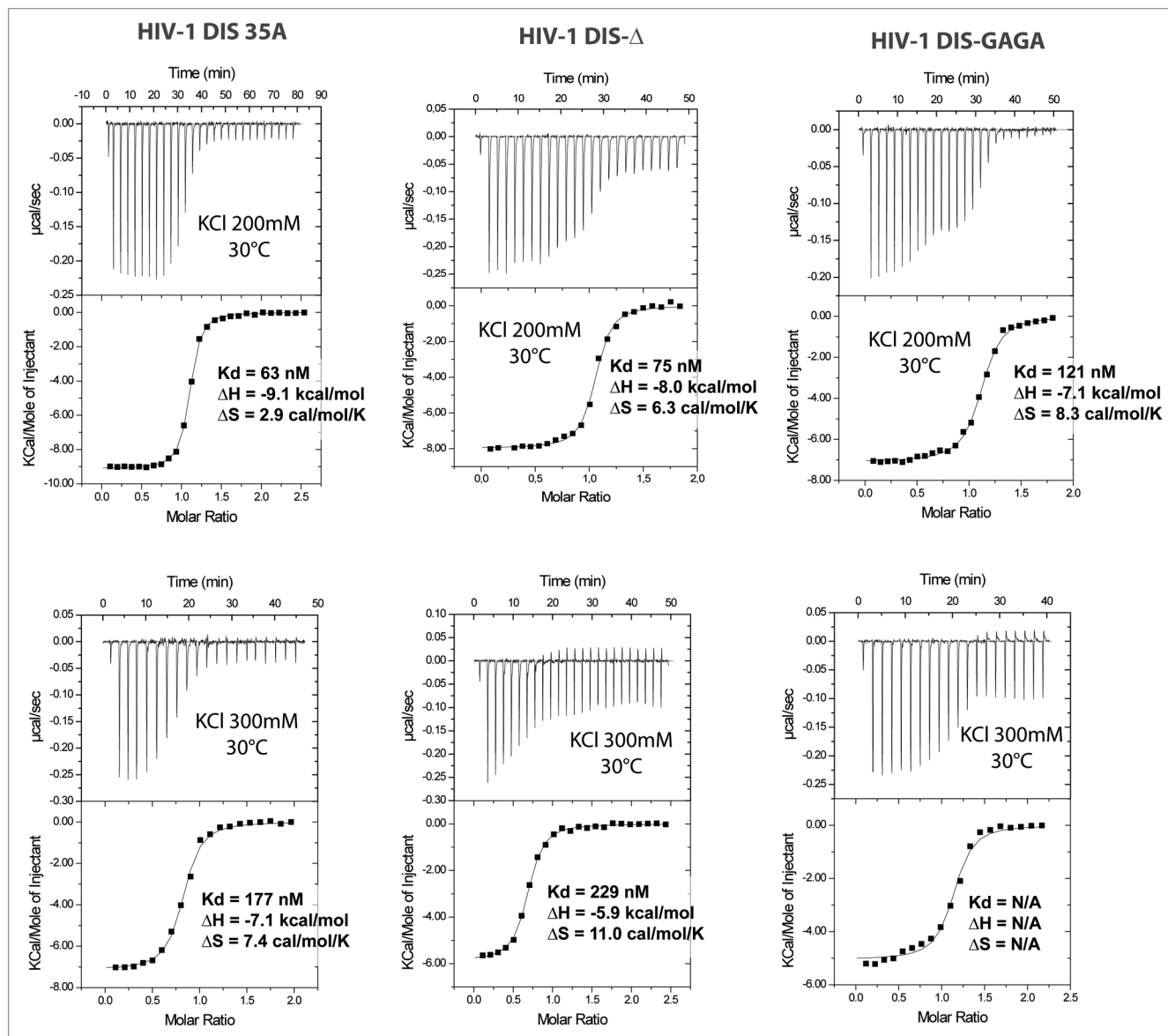


Figure 5. ITC profiles for the titration of HIV-1 Vif on the HIV-1 DIS loop-loop complex and mutant DIS sequences at 30°C and in presence of 200 or 300 mM of KCl. Each heat burst curve is the result of a 1.5 or 2.0 μ l injection of 200 μ M Vif in a 15 μ M RNA solution. The corrected injection heats were derived by integration of the ITC profiles and were fitted with a one site binding model. N/A. denotes “not applicable” since accurate values could not be obtained using a single site binding model.

compounds have been reported to block the Tat/TAR interaction in vitro and in infected cells with inhibition constants in the low nanomolar-range by competing with Tat for binding to the TAR UCU bulge.⁷⁰⁻⁷³ We can therefore postulate that such compounds should also interfere with the binding of Vif to TAR (Fig. 6A). This hypothesis however remains to be tested.

Regarding the DIS RNA, our results show that Vif interacts both with the loop-loop helix and the 7-base-pair stem adjacent to the apical loop. Interestingly, it was shown that this stem is important for APOBEC3G binding to the viral RNA.⁷⁴ An attractive hypothesis is therefore that Vif could compete with APOBEC3G for binding the DIS, thus physically excluding the antiviral factor from packaging (Fig. 6B). Finally, we have

previously shown that some 4,5-disubstituted aminoglycoside antibiotics specifically and tightly bind DIS dimers through interactions with the loop-loop helix and stem.^{57,75-78} We therefore plan in a next future to investigate a putative interference of such aminoglycosides on the Vif/DIS interaction.

Materials and Methods

Expression and purification of recombinant Vif. A polymerase chain reaction (PCR) on the pcDNA-HVif vector encoding the full-length HIV-1 NL4-3 Vif protein⁷⁹ was used to amplify the Vif gene and to insert *Nde*I and *Bam*HI restriction sites at the extremities. The digested PCR product was then inserted between

*Nde*I and *Bam*HI sites into the bacterial expression plasmid pNEAtH⁸⁰ encoding a 6-His tag followed by a thrombin cleavage site, leading to a Vif construct containing a histidine tag and a protease cleavage site fused with the Vif N terminus (MGS SHH HHH HSS GTG SGL VPR GSH-Vif). The sequence of the Vif protein used is shown on **Supplemental Figures**. These plasmids pNEAtH-Vif were used to chemically transform *E. coli* Rosetta 2 strains. Production of Vif proteins was induced in LB liquid medium by addition of 0.5 mM IPTG to log phase bacterial culture (OD 600 nm = 0.5–0.6). After 4 h at 37°C bacteria were harvested by centrifugation at 4,000 g during 15 min and lysed by an overnight stirring at room temperature in the denaturing buffer (6 M guanidine Hydrochloride, 100 mM sodium phosphate, 50 mM Tris, pH 8.0). Cellular debris were separated by centrifugation at 100,000 g during 1 h at 4°C and the cleared lysate was loaded onto a Ni-NTA agarose column. The column was washed with the lysis buffer and elution was performed by applying 25 ml of the same solution at decreasing pH values (pH 6.5, pH 6.0, pH 5.8, pH 5.5 and pH 5.0). The Vif containing fractions were identified on a 12% SDS-PAGE, pooled and the volume was completed to 50 ml (~0.3 mg ml⁻¹ of Vif) using elution buffer. The protein was renaturated by successive dialysis for 1 h at 4°C against 500 ml of a buffer containing 50 mM MOPS pH 6.5, 150 mM NaCl, 10% glycerol, 1 mM dithiothreitol and decreasing guanidium chloride concentrations (3.0 M, 1.5 M, 0.75 M, 0.42 M, 0.21 M and finally 0 M). The protein was then concentrated to ~5 mg ml⁻¹ on an Amicon Ultra-10 and stored at -80°C. Stock solutions were centrifuged at 100,000 g for 1 h immediately prior to use. The molecular mass of the purified protein was checked by mass spectrometry (Calculated mass: 25,035 Da, Observed mass: 25,036 Da, see **Fig. S3A**) and the identity of the protein was assessed by peptide mass fingerprinting (PMF, see **Fig. S3B**). The purified protein was > 95% pure based on SDS-PAGE analysis (**Fig. S4**).

Prior measurements, Vif was dialysed in either the ITC buffer (50 mM MOPS pH 6.5, 200–300 mM KCl, 2 mM MgCl₂, 10% glycerol, 1 mM dithiothreitol) or the CD buffer [50 mM MOPS pH 6.5, 150 mM NaCl, 2.5% glycerol, 1 mM tris(2-carboxyethyl)phosphine]. The protein was then concentrated to 100 μM for CD and 150–280 μM for ITC measurements. All buffers were argon-degassed.

Mass spectrometry. Protein samples were dialyzed against 200 mM ammonium acetate and subsequently diluted in 1:10 water acetonitrile (v/v) mixture acidified with 1% formic acid to achieve a concentration of 0.3 M. Mass spectrometry was performed on an ESI-TOF mass spectrometer Q-TOF micro (Waters, MA USA). Calibration was achieved in the positive ion mode, using denatured horse heart myoglobin (Sigma), using denatured horse heart myoglobin (Sigma). For PMF analysis, Vif (10 μl, 5 mg ml⁻¹) was digested with trypsin (1 μl, 10 ng μl⁻¹) in native conditions in 50 mM ammonium carbonate for 30 min at

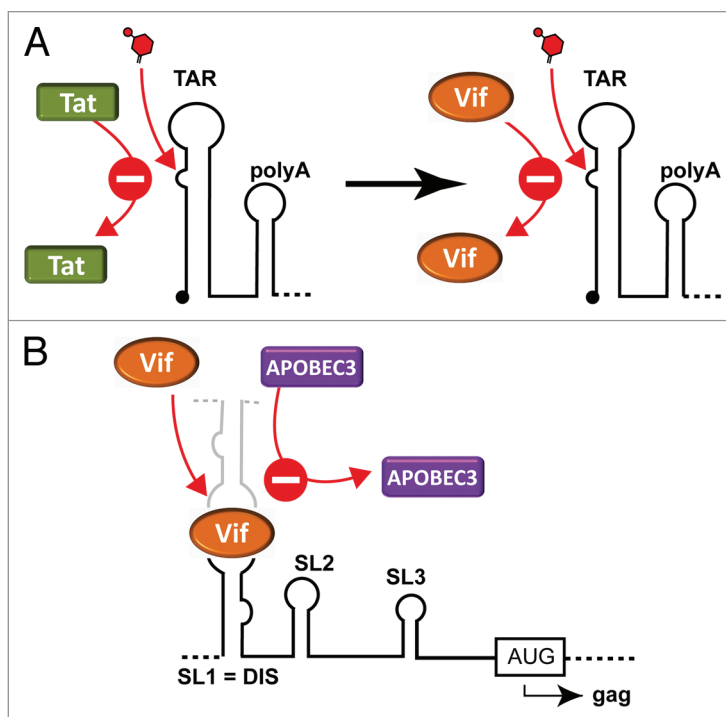


Figure 6. Consequences of our results for Vif-RNA interactions. (A) The HIV-1 Tat protein is known to bind the TAR lateral bulge. Small molecules are known to prevent this binding by inhibiting the Tat binding. Since Vif also recognizes the TAR lateral bulge, we anticipate that such Tat/TAR inhibitors could also prevent Vif binding to TAR. (B) Scheme showing that Vif could reduce APOBEC3 binding to the viral genome by competing for the DIS sequence.

37°C. Data were collected on an Autoflex III MALDI-TOF mass spectrometer (Bruker).

Light scattering experiments. Dynamic Light Scattering (DLS) was performed using a Zetasizer Nano S (Malvern). Static Light Scattering (SLS) was performed on a Dynapro Nanostar (Wyatt Technology Europe). For DLS experiments, protein sample was adjusted to 200 μM in the buffer 50 mM MOPS, pH 6.5, 150 mM NaCl, 0–10% glycerol, 1 mM dithiothreitol. For SLS experiments, a 0.1 mg ml⁻¹ protein concentration was used in the same buffer containing 5% glycerol. Sample temperature was maintained at 30°C. Fluctuations of the scattered intensity due to Brownian motions were recorded at microsecond time intervals. An autocorrelation function was derived, thus leading to the determination of diffusion coefficients. Assimilating proteins in solution to spheres, diffusion coefficients were related to the hydrodynamic radius of the particles, R_h via the Stokes-Einstein equation:

$$D = k_B T / 6\pi\eta R_h$$

where k_B is the Boltzmann constant, T the temperature, η the solvent viscosity and D the translational diffusion coefficient. All experimental data were corrected for solvent viscosity using an AMVn automated micro viscosimeter (Anton Paar) and for refractive index using an Abbé refractometer. Data were analyzed using DLS analysis software (Malvern).

Circular dichroism. Vif protein sample was prepared in 50 mM MOPS, 150 mM NaCl, 2.5% glycerol, 1 mM tris(2-carboxyethyl)phosphine, at a concentration of 100 μ M and diluted again in the same buffer prior to the experiment at a final concentration of 25 μ M. Far-UV CD measurements were performed with a J-850 Jasco spectropolarimeter equipped with a Peltier temperature controller and calibrated with ammonium d-10 camphorsulfonate. Spectra (186–260 nm) were measured at 30°C, with a constant bandwidth of 1 nm and a 3–5 sec integration time using a quartz cell of path length 0.1 mm. Spectra were averaged over ten scans and corrected for buffer contributions. Quantitative estimations of the secondary structure contents were performed using Dichroweb⁸¹ and the reference CDSSTR database 4 containing the CD spectra of 43 soluble proteins ranging from 190 to 240 nm.

RNA sample preparation. Chemically-synthesized wild-type HIV-1 subtype B 27-mer TAR RNA, HIV-1 subtype A 35-mer DIS RNA, 27-mer Sarcin-Ricin Loop (SRL) from the *E. coli* 23 S rRNA, as well as TAR and DIS mutant sequences were purchased from Integrated DNA technologies or from Dharmacon. RNA were purified as described in reference 82. In short, RNA was loaded on a Nucleopac PA-100 column (Dionex) heated at 70°C equilibrated in 4 M urea, 20 mM Mes [2-N(-Morpholine) ethane sulfonic acid], pH 6.2 and eluted using a NaClO₄ gradient.

DIS kissing-loop complexes were obtained as follows: RNA was diluted to 2 μ M concentration in water, heated at 90°C for 5 min and then cooled on ice for 5 min. As shown previously, this protocol essentially leads to the formation of DIS loop-loop dimers and prevents the formation of extended duplex dimers.^{83,84} A similar protocol was performed for folding of TAR and SRL hairpins. DIS-A272U/ Δ G273 was diluted to 60 μ M in water, heated at 90°C for 5 min and then cooled at room temperature. This protocol was used in order to favor the formation of a duplex instead of hairpin monomers. Folding buffer (50 mM MOPS pH 6.5, 200 mM KCl, 2 mM MgCl₂) was then added and RNA samples were dialysed against ITC buffer (50 mM MOPS pH 6.5, 200–300 mM KCl, 2 mM MgCl₂, 10% glycerol, 1 mM dithiothreitol) and adjusted to a final concentration of 15 μ M.

Isothermal titration calorimetry (ITC). ITC measurements were performed on a MicroCal ITC₂₀₀ (GE Healthcare) in ITC buffer containing 200 or 300 mM KCl. In a typical experiment,

27 injections of 1.5 μ l aliquots of Vif protein at 150–280 μ M were injected (at 0.5 μ l s⁻¹) into 203 μ l of RNA at 15 μ M in the sample cell. The delay between injections was 120 sec. All ITC curves were analyzed using the software Origin (OriginLab). All data could be fitted with a single-site model. Standard free energies of binding (Δ G) were obtained using the equation

$$\Delta G = -RT \ln K_a$$

Entropic contributions were obtained from the relationship

$$\Delta G = \Delta H - T \Delta S$$

In our experimental conditions, the product $K_a \times [\text{RNA}] \times N$, where N is the number of binding sites, was in the 0.1–1,000 range, allowing an accurate and simultaneous determination of binding parameters by ITC.⁵⁶ Because of a too fast Vif-RNA binding, it was not possible to use our recently-developed *kinITC* approach to derive kinetic parameters of binding in addition to thermodynamic data.⁸⁵

Disclosure of Potential Conflicts of Interest

No potential conflicts of interest were disclosed.

Acknowledgements

We thank Dr Bernard Lorber for his assistance in D.L.S. and S.L.S. experiments, Dr Guillaume Bec and Guillaume Hoffmann for their technical assistance, Dr Carine Tisé and Dr Serena Bernacchi for fruitful discussions and comments. The following reagent was obtained through the NIH AIDS Research and Reference Reagent Program, Division of AIDS, NIAID, NIH: pcDNA-HVif from Dr Stephan Bour and Dr Klaus Strebelt.

Funding

This work was supported by the “Agence Nationale de Recherche sur le SIDA” (ANRS to E.E.). S.F. is an ANRS fellow. J.M. is a SIDACTION/Fondation Pierre Bergé fellow.

Supplemental Materials

Supplemental materials may be found here: www.landesbioscience.com/journals/rnabiology/article/20483

References

- Fisher AG, Ensoli B, Ivanoff L, Chamberlain M, Petteway S, Ratner L, et al. The sor gene of HIV-1 is required for efficient virus transmission in vitro. *Science* 1987; 237:888-93; PMID:3497453; <http://dx.doi.org/10.1126/science.3497453>.
- Gabuzda DH, Lawrence K, Langhoff E, Terwilliger E, Dorfman T, Haseltine WA, et al. Role of vif in replication of human immunodeficiency virus type 1 in CD4⁺ T lymphocytes. *J Virol* 1992; 66:6489-95; PMID:1357189.
- Gallo R, Wong-Staal F, Montagnier L, Haseltine WA, Yoshida M. HIV/HTLV gene nomenclature. *Nature* 1988; 333:504; PMID:2836736; <http://dx.doi.org/10.1038/333504a0>.
- Sodroski J, Goh WC, Rosen C, Tartar A, Portetelle D, Burny A, et al. Replicative and cytopathic potential of HTLV-III/LAV with sor gene deletions. *Science* 1986; 231:1549-53; PMID:3006244; <http://dx.doi.org/10.1126/science.3006244>.
- Strebelt K, Daugherty D, Clouse K, Cohen D, Folks T, Martin MA. The HIV 'A' (sor) gene product is essential for virus infectivity. *Nature* 1987; 328:728-30; PMID:2441266; <http://dx.doi.org/10.1038/328728a0>.
- Harris RS, Bishop KN, Sheehy AM, Craig HM, Petersen-Mahrt SK, Watt IN, et al. DNA deamination mediates innate immunity to retroviral infection. *Cell* 2003; 113:803-9; PMID:12809610; [http://dx.doi.org/10.1016/S0092-8674\(03\)00423-9](http://dx.doi.org/10.1016/S0092-8674(03)00423-9).
- Zhang H, Yang B, Pomerantz RJ, Zhang C, Arunachalam SC, Gao L. The cytidine deaminase CEM15 induces hypermutation in newly synthesized HIV-1 DNA. *Nature* 2003; 424:94-8; PMID:12808465; <http://dx.doi.org/10.1038/nature01707>.
- Mangeat B, Turelli P, Caron G, Friedli M, Perrin L, Trono D. Broad antiretroviral defence by human APOBEC3G through lethal editing of nascent reverse transcripts. *Nature* 2003; 424:99-103; PMID:12808466; <http://dx.doi.org/10.1038/nature01709>.
- Bishop KN, Holmes RK, Malim MH. Antiviral potency of APOBEC proteins does not correlate with cytidine deamination. *J Virol* 2006; 80:8450-8; PMID:16912295; <http://dx.doi.org/10.1128/JVI.00839-06>.
- Bishop KN, Verma M, Kim EY, Wolinsky SM, Malim MH. APOBEC3G inhibits elongation of HIV-1 reverse transcripts. *PLoS Pathog* 2008; 4:1000231; PMID:19057663; <http://dx.doi.org/10.1371/journal.ppat.1000231>.
- Holmes RK, Malim MH, Bishop KN. APOBEC-mediated viral restriction: not simply editing? *Trends Biochem Sci* 2007; 32:118-28; PMID:17303427; <http://dx.doi.org/10.1016/j.tibs.2007.01.004>.

12. Bishop KN, Holmes RK, Sheehy AM, Davidson NO, Cho SJ, Malim MH. Cytidine deamination of retroviral DNA by diverse APOBEC proteins. *Curr Biol* 2004; 14:1392-6; PMID:15296758; <http://dx.doi.org/10.1016/j.cub.2004.06.057>.
13. Sheehy AM, Gaddis NC, Choi JD, Malim MH. Isolation of a human gene that inhibits HIV-1 infection and is suppressed by the viral Vif protein. *Nature* 2002; 418:646-50; PMID:12167863; <http://dx.doi.org/10.1038/nature00939>.
14. Wiegand HL, Doehle BP, Bogerd HP, Cullen BR. A second human antiretroviral factor, APOBEC3F, is suppressed by the HIV-1 and HIV-2 Vif proteins. *EMBO J* 2004; 23:2451-8; PMID:15152192; <http://dx.doi.org/10.1038/sj.emboj.7600246>.
15. Zheng YH, Irwin D, Kurosu T, Tokunaga K, Sata T, Peterlin BM. Human APOBEC3F is another host factor that blocks human immunodeficiency virus type 1 replication. *J Virol* 2004; 78:6073-6; PMID:15141007; <http://dx.doi.org/10.1128/JVI.78.11.6073-6.2004>.
16. Doehle BP, Schäfer A, Cullen BR. Human APOBEC3B is a potent inhibitor of HIV-1 infectivity and is resistant to HIV-1 Vif. *Virology* 2005; 339:281-8; PMID:15993456; <http://dx.doi.org/10.1016/j.virol.2005.06.005>.
17. Dang Y, Wang X, Esselman WJ, Zheng YH. Identification of APOBEC3DE as another antiretroviral factor from the human APOBEC family. *J Virol* 2006; 80:10522-33; PMID:16920826; <http://dx.doi.org/10.1128/JVI.01123-06>.
18. Dang Y, Siew LM, Wang X, Han Y, Lampen R, Zheng YH. Human cytidine deaminase APOBEC3H restricts HIV-1 replication. *J Biol Chem* 2008; 283:11606-14; PMID:18299330; <http://dx.doi.org/10.1074/jbc.M707586200>.
19. Stenglein MD, Harris RS. APOBEC3B and APOBEC3F inhibit L1 retrotransposition by a DNA deamination-independent mechanism. *J Biol Chem* 2006; 281:16837-41; PMID:16648136; <http://dx.doi.org/10.1074/jbc.M602367200>.
20. OhAinle M, Kerns JA, Malik HS, Emerman M. Adaptive evolution and antiviral activity of the conserved mammalian cytidine deaminase APOBEC3H. *J Virol* 2006; 80:3853-62; PMID:16571802; <http://dx.doi.org/10.1128/JVI.80.8.3853-62.2006>.
21. Chiu YL, Greene WC. The APOBEC3 cytidine deaminases: an innate defensive network opposing exogenous retroviruses and endogenous retroelements. *Annu Rev Immunol* 2008; 26:317-53; PMID:18304004; <http://dx.doi.org/10.1146/annurev.immunol.26.021607.090350>.
22. Henriot S, Mercenne G, Bernacchi S, Paillart JC, Marquet R. Tumultuous relationship between the human immunodeficiency virus type 1 viral infectivity factor (Vif) and the human APOBEC-3G and APOBEC-3F restriction factors. *Microbiol Mol Biol Rev* 2009; 73:211-32; PMID:19487726; <http://dx.doi.org/10.1128/MMBR.00040-08>.
23. Wissing S, Galloway NL, Greene WC. HIV-1 Vif versus the APOBEC3 cytidine deaminases: an intracellular duel between pathogen and host restriction factors. *Mol Aspects Med* 2010; 31:383-97; PMID:20538015; <http://dx.doi.org/10.1016/j.mam.2010.06.001>.
24. Conticello SG, Harris RS, Neuberger MS. The Vif protein of HIV triggers degradation of the human antiretroviral DNA deaminase APOBEC3G. *Curr Biol* 2003; 13:2009-13; PMID:14614829; <http://dx.doi.org/10.1016/j.cub.2003.10.034>.
25. Marin M, Rose KM, Kozak SL, Kabat D. HIV-1 Vif protein binds the editing enzyme APOBEC3G and induces its degradation. *Nat Med* 2003; 9:1398-403; PMID:14528301; <http://dx.doi.org/10.1038/nm946>.
26. Mehle A, Strack B, Ancuta P, Zhang C, McPike M, Gabuzda D. Vif overcomes the innate antiviral activity of APOBEC3G by promoting its degradation in the ubiquitin-proteasome pathway. *J Biol Chem* 2004; 279:7792-8; PMID:14672928; <http://dx.doi.org/10.1074/jbc.M313093200>.
27. Sheehy AM, Gaddis NC, Malim MH. The antiretroviral enzyme APOBEC3G is degraded by the proteasome in response to HIV-1 Vif. *Nat Med* 2003; 9:1404-7; PMID:14528300; <http://dx.doi.org/10.1038/nm945>.
28. Stopak K, de Noronha C, Yonemoto W, Greene WC. HIV-1 Vif blocks the antiviral activity of APOBEC3G by impairing both its translation and intracellular stability. *Mol Cell* 2003; 12:591-601; PMID:14527406; [http://dx.doi.org/10.1016/S1097-2765\(03\)00353-8](http://dx.doi.org/10.1016/S1097-2765(03)00353-8).
29. Hultquist JF, Binka M, LaRue RS, Simon V, Harris RS. Vif proteins of human and simian immunodeficiency viruses require cellular CBF β to degrade APOBEC3 restriction factors. *J Virol* 2012; 86:2874-7; PMID:22205746; <http://dx.doi.org/10.1128/JVI.06950-11>.
30. Jäger S, Kim DY, Hultquist JF, Shindo K, LaRue RS, Kwon E, et al. Vif hijacks CBF β to degrade APOBEC3G and promote HIV-1 infection. *Nature* 2012; 481:371-5; PMID:22190037.
31. Zhang W, Du J, Evans SL, Yu Y, Xu XF. T-cell differentiation factor CBF β regulates HIV-1 Vif-mediated evasion of host restriction. *Nature* 2012; 481:376-9; PMID:22190036.
32. Kao S, Khan MA, Miyagi E, Plishka R, Buckler-White A, Strebel K. The human immunodeficiency virus type 1 Vif protein reduces intracellular expression and inhibits packaging of APOBEC3G (CEM15), a cellular inhibitor of virus infectivity. *J Virol* 2003; 77:11398-407; PMID:14557625; <http://dx.doi.org/10.1128/JVI.77.21.11398-407.2003>.
33. Mercenne G, Bernacchi S, Richer D, Bec G, Henriot S, Paillart JC, et al. HIV-1 Vif binds to APOBEC3G mRNA and inhibits its translation. *Nucleic Acids Res* 2010; 38:633-46; PMID:19910370; <http://dx.doi.org/10.1093/nar/gkp1009>.
34. Mariani R, Chen D, Schröfelbauer B, Navarro F, König R, Bollman B, et al. Species-specific exclusion of APOBEC3G from HIV-1 virions by Vif. *Cell* 2003; 114:21-31; PMID:12859895; [http://dx.doi.org/10.1016/S0092-8674\(03\)00515-4](http://dx.doi.org/10.1016/S0092-8674(03)00515-4).
35. Opi S, Kao S, Goila-Gaur R, Khan MA, Miyagi E, Takeuchi H, et al. Human immunodeficiency virus type 1 Vif inhibits packaging and antiviral activity of a degradation-resistant APOBEC3G variant. *J Virol* 2007; 81:8236-46; PMID:17522211; <http://dx.doi.org/10.1128/JVI.02694-06>.
36. Dettenhofer M, Cen S, Carlson BA, Kleiman L, Yu XF. Association of human immunodeficiency virus type 1 Vif with RNA and its role in reverse transcription. *J Virol* 2000; 74:8938-45; PMID:10982337; <http://dx.doi.org/10.1128/JVI.74.19.8938-45.2000>.
37. Henriot S, Richer D, Bernacchi S, Decroly E, Vigne R, Ehresmann B, et al. Cooperative and specific binding of Vif to the 5' region of HIV-1 genomic RNA. *J Mol Biol* 2005; 354:55-72; PMID:16236319; <http://dx.doi.org/10.1016/j.jmb.2005.09.025>.
38. Khan MA, Akari H, Kao S, Aberham C, Davis D, Buckler-White A, et al. Intravirion processing of the human immunodeficiency virus type 1 Vif protein by the viral protease may be correlated with Vif function. *J Virol* 2002; 76:9112-23; PMID:12186895; <http://dx.doi.org/10.1128/JVI.76.18.9112-23.2002>.
39. Zhang H, Pomerantz RJ, Dornadula G, Sun Y. Human immunodeficiency virus type 1 Vif protein is an integral component of an mRNP complex of viral RNA and could be involved in the viral RNA folding and packaging process. *J Virol* 2000; 74:8252-61; PMID:10954522; <http://dx.doi.org/10.1128/JVI.74.18.8252-61.2000>.
40. Barraud P, Paillart JC, Marquet R, Tisné C. Advances in the structural understanding of Vif proteins. *Curr HIV Res* 2008; 6:91-9; PMID:18336256; <http://dx.doi.org/10.2174/157016208783885056>.
41. Bernacchi S, Henriot S, Dumas P, Paillart JC, Marquet R. RNA and DNA binding properties of HIV-1 Vif protein: a fluorescence study. *J Biol Chem* 2007; 282:26361-8; PMID:17609216; <http://dx.doi.org/10.1074/jbc.M70312200>.
42. Bernacchi S, Mercenne G, Tournaire C, Marquet R, Paillart JC. Importance of the proline-rich multimerization domain on the oligomerization and nucleic acid binding properties of HIV-1 Vif. *Nucleic Acids Res* 2011; 39:2404-15; PMID:21076154; <http://dx.doi.org/10.1093/nar/gkq979>.
43. Auclair JR, Green KM, Shandilya S, Evans JE, Somasundaran M, Schiffer CA. Mass spectrometry analysis of HIV-1 Vif reveals an increase in ordered structure upon oligomerization in regions necessary for viral infectivity. *Proteins* 2007; 69:270-84; PMID:17598142; <http://dx.doi.org/10.1002/prot.21471>.
44. Yang S, Sun Y, Zhang H. The multimerization of human immunodeficiency virus type I Vif protein: a requirement for Vif function in the viral life cycle. *J Biol Chem* 2001; 276:4889-93; PMID:11071884; <http://dx.doi.org/10.1074/jbc.M004895200>.
45. Donahue JP, Vetter ML, Mukhtar NA, D'Aquila RT. The HIV-1 Vif PPLP motif is necessary for human APOBEC3G binding and degradation. *Virology* 2008; 377:49-53; PMID:18499212; <http://dx.doi.org/10.1016/j.virol.2008.04.017>.
46. Miller JH, Presnyak V, Smith HC. The dimerization domain of HIV-1 viral infectivity factor Vif is required to block virion incorporation of APOBEC3G. *Retrovirology* 2007; 4:81; PMID:18036235; <http://dx.doi.org/10.1186/1742-4690-4-81>.
47. Yang B, Gao L, Li L, Lu Z, Fan X, Patel CA, et al. Potent suppression of viral infectivity by the peptides that inhibit multimerization of human immunodeficiency virus type 1 (HIV-1) Vif proteins. *J Biol Chem* 2003; 278:6596-602; PMID:12480936; <http://dx.doi.org/10.1074/jbc.M210164200>.
48. Bergeron JR, Huthoff H, Veselkov DA, Bevil RL, Simpson PJ, Matthews SJ, et al. The SOCS-box of HIV-1 Vif interacts with ElonginBC by induced-folding to recruit its Cul5-containing ubiquitin ligase complex. *PLoS Pathog* 2010; 6:1000925; PMID:20532212; <http://dx.doi.org/10.1371/journal.ppat.1000925>.
49. Gallerano D, Devanaboyina SC, Swoboda I, Linhart B, Mittermann I, Keller W, et al. Biophysical characterization of recombinant HIV-1 subtype C virus infectivity factor. *Amino Acids* 2011; 40:981-9; PMID:20809132; <http://dx.doi.org/10.1007/s00726-010-0725-x>.
50. Yang X, Goncalves J, Gabuzda D. Phosphorylation of Vif and its role in HIV-1 replication. *J Biol Chem* 1996; 271:10121-9; PMID:8626571; <http://dx.doi.org/10.1074/jbc.271.17.10121>.
51. Marcisin SR, Engen JR. Molecular insight into the conformational dynamics of the Elongin BC complex and its interaction with HIV-1 Vif. *J Mol Biol* 2010; 402:892-904; PMID:20728451; <http://dx.doi.org/10.1016/j.jmb.2010.08.026>.
52. Marcisin SR, Narute PS, Emert-Sedlak LA, Kloczewiak M, Smithgall TE, Engen JR. On the solution conformation and dynamics of the HIV-1 viral infectivity factor. *J Mol Biol* 2011; 410:1008-22; PMID:21763503; <http://dx.doi.org/10.1016/j.jmb.2011.04.053>.
53. Paul I, Cui J, Maynard EL. Zinc binding to the HCCH motif of HIV-1 virion infectivity factor induces a conformational change that mediates protein-protein interactions. *Proc Natl Acad Sci USA* 2006; 103:18475-80; PMID:17132731; <http://dx.doi.org/10.1073/pnas.0604150103>.
54. Feig AL. Studying RNA-RNA and RNA-protein interactions by isothermal titration calorimetry. *Methods Enzymol* 2009; 468:409-22; PMID:20946780; [http://dx.doi.org/10.1016/S0076-6879\(09\)68019-8](http://dx.doi.org/10.1016/S0076-6879(09)68019-8).
55. Salim NN, Feig AL. Isothermal titration calorimetry of RNA. *Methods* 2009; 47:198-205; PMID:18835447; <http://dx.doi.org/10.1016/j.ymeth.2008.09.003>.
56. Velázquez Campoy A, Freire E. ITC in the post-genomic era...? Pricelless. *Biophys Chem* 2005; 115:115-24; PMID:15752592; <http://dx.doi.org/10.1016/j.bpc.2004.12.015>.

57. Ennifar E, Paillart JC, Bernacchi S, Walter P, Pale P, Decout JL, et al. A structure-based approach for targeting the HIV-1 genomic RNA dimerization initiation site. *Biochimie* 2007; 89:1195-203; PMID:17434658; <http://dx.doi.org/10.1016/j.biochi.2007.03.003>.
58. Paillart JC, Shehu-Xhilaga M, Marquet R, Mak J. Dimerization of retroviral RNA genomes: an inseparable pair. *Nat Rev Microbiol* 2004; 2:461-72; PMID:15152202; <http://dx.doi.org/10.1038/nrmicro903>.
59. Shen N, Jetté L, Wainberg MA, Laughrea M. Role of stem B, loop B and nucleotides next to the primer binding site and the kissing-loop domain in human immunodeficiency virus type 1 replication and genomic-RNA dimerization. *J Virol* 2001; 75:10543-9; PMID:11581429; <http://dx.doi.org/10.1128/JVI.75.21.10543-9.2001>.
60. Hagan NA, Fabris D. Dissecting the protein-RNA and RNA-RNA interactions in the nucleocapsid-mediated dimerization and isomerization of HIV-1 stemloop 1. *J Mol Biol* 2007; 365:396-410; PMID:17070549; <http://dx.doi.org/10.1016/j.jmb.2006.09.081>.
61. Ennifar E, Dumas P. Polymorphism of bulged-out residues in HIV-1 RNA DIS kissing complex and structure comparison with solution studies. *J Mol Biol* 2006; 356:771-82; PMID:16403527; <http://dx.doi.org/10.1016/j.jmb.2005.12.022>.
62. Ennifar E, Walter P, Ehresmann B, Ehresmann C, Dumas P. Crystal structures of coaxially stacked kissing complexes of the HIV-1 RNA dimerization initiation site. *Nat Struct Biol* 2001; 8:1064-8; PMID:11702070; <http://dx.doi.org/10.1038/nsb727>.
63. Ennifar E, Walter P, Dumas P. Cation-dependent cleavage of the duplex form of the subtype-B HIV-1 RNA dimerization initiation site. *Nucleic Acids Res* 2010; 38:5807-16; PMID:20460458; <http://dx.doi.org/10.1093/nar/gkq344>.
64. Ennifar E, Yusupov M, Walter P, Marquet R, Ehresmann B, Ehresmann C, et al. The crystal structure of the dimerization initiation site of genomic HIV-1 RNA reveals an extended duplex with two adenine bulges. *Structure* 1999; 7:1439-49; PMID:10574792; [http://dx.doi.org/10.1016/S0969-2126\(00\)80033-7](http://dx.doi.org/10.1016/S0969-2126(00)80033-7).
65. Muriaux D, De Rocquigny H, Roques BP, Paoletti J. NCp7 activates HIV-1 RNA dimerization by converting a transient loop-loop complex into a stable dimer. *J Biol Chem* 1996; 271:33686-92; PMID:8969239; <http://dx.doi.org/10.1074/jbc.271.52.33686>.
66. Takahashi KI, Baba S, Chattopadhyay P, Koyanagi Y, Yamamoto N, Takaku H, et al. Structural requirement for the two-step dimerization of human immunodeficiency virus type 1 genome. *RNA* 2000; 6:96-102; PMID:10668802; <http://dx.doi.org/10.1017/S1355838200991635>.
67. Roy S, Delling U, Chen CH, Rosen CA, Sonenberg N. A bulge structure in HIV-1 TAR RNA is required for Tat binding and Tat-mediated trans-activation. *Genes Dev* 1990; 4:1365-73; PMID:2227414; <http://dx.doi.org/10.1101/gad.4.8.1365>.
68. Weeks KM, Ampe C, Schultz SC, Steitz TA, Crothers DM. Fragments of the HIV-1 Tat protein specifically bind TAR RNA. *Science* 1990; 249:1281-5; PMID:2205002; <http://dx.doi.org/10.1126/science.2205002>.
69. Karn J. Tackling Tat. *J Mol Biol* 1999; 293:235-54; PMID:10550206; <http://dx.doi.org/10.1006/jmbi.1999.3060>.
70. Davis B, Afshar M, Varani G, Murchie AI, Karn J, Lentzen G, et al. Rational design of inhibitors of HIV-1 TAR RNA through the stabilisation of electrostatic "hot spots". *J Mol Biol* 2004; 336:343-56; PMID:14757049; <http://dx.doi.org/10.1016/j.jmb.2003.12.046>.
71. Hamy F, Felder ER, Heizmann G, Lazdins J, Aboul-ela F, Varani G, et al. An inhibitor of the Tat/TAR RNA interaction that effectively suppresses HIV-1 replication. *Proc Natl Acad Sci USA* 1997; 94:3548-53; PMID:9108013; <http://dx.doi.org/10.1073/pnas.94.8.3548>.
72. Lalonde MS, Lobritz MA, Ratcliff A, Chamanian M, Athanassiou Z, Tyagi M, et al. Inhibition of both HIV-1 reverse transcription and gene expression by a cyclic peptide that binds the Tat-transactivating response element (TAR) RNA. *PLoS Pathog* 2011; 7:1002038; PMID:21625572; <http://dx.doi.org/10.1371/journal.ppat.1002038>.
73. Mei HY, Mack DP, Galan AA, Halim NS, Heldsinger A, Loo JA, et al. Discovery of selective, small-molecule inhibitors of RNA complexes-I. The Tat protein/TAR RNA complexes required for HIV-1 transcription. *Bioorg Med Chem* 1997; 5:1173-84; PMID:9222511; [http://dx.doi.org/10.1016/S0968-0896\(97\)00064-3](http://dx.doi.org/10.1016/S0968-0896(97)00064-3).
74. Khan MA, Kao S, Miyagi E, Takeuchi H, Goila-Gaur R, Opi S, et al. Viral RNA is required for the association of APOBEC3G with human immunodeficiency virus type 1 nucleoprotein complexes. *J Virol* 2005; 79:5870-4; PMID:15827203; <http://dx.doi.org/10.1128/JVI.79.9.5870-4.2005>.
75. Bernacchi S, Freisz S, Maechling C, Spiess B, Marquet R, Dumas P, et al. Aminoglycoside binding to the HIV-1 RNA dimerization initiation site: thermodynamics and effect on the kissing-loop to duplex conversion. *Nucleic Acids Res* 2007; 35:7128-39; PMID:17942426; <http://dx.doi.org/10.1093/nar/gkm856>.
76. Ennifar E, Paillart JC, Bodlener A, Walter P, Weibel JM, Aubertin AM, et al. Targeting the dimerization initiation site of HIV-1 RNA with aminoglycosides: from crystal to cell. *Nucleic Acids Res* 2006; 34:2328-39; PMID:16679451; <http://dx.doi.org/10.1093/nar/gkl317>.
77. Ennifar E, Paillart JC, Marquet R, Ehresmann B, Ehresmann C, Dumas P, et al. HIV-1 RNA dimerization initiation site is structurally similar to the ribosomal A site and binds aminoglycoside antibiotics. *J Biol Chem* 2003; 278:2723-30; PMID:12435744; <http://dx.doi.org/10.1074/jbc.M205726200>.
78. Freisz S, Lang K, Micura R, Dumas P, Ennifar E. Binding of aminoglycoside antibiotics to the duplex form of the HIV-1 genomic RNA dimerization initiation site. *Angew Chem Int Ed Engl* 2008; 47:4110-3; PMID:18435520; <http://dx.doi.org/10.1002/anie.200800726>.
79. Nguyen KL, llano M, Akari H, Miyagi E, Poeschla EM, Strebel K, et al. Codon optimization of the HIV-1 vpu and vif genes stabilizes their mRNA and allows for highly efficient Rev-independent expression. *Virology* 2004; 319:163-75; PMID:15015498; <http://dx.doi.org/10.1016/j.virol.2003.11.021>.
80. Romier C, Ben Jelloul M, Albeck S, Buchwald G, Busso D, Celie PH, et al. Co-expression of protein complexes in prokaryotic and eukaryotic hosts: experimental procedures, database tracking and case studies. *Acta Crystallogr D Biol Crystallogr* 2006; 62:1232-42; PMID:17001100; <http://dx.doi.org/10.1107/S0907444906031003>.
81. Whitmore L, Wallace BA. Protein secondary structure analyses from circular dichroism spectroscopy: methods and reference databases. *Biopolymers* 2008; 89:392-400; PMID:17896349; <http://dx.doi.org/10.1002/bip.20853>.
82. Ennifar E, Walter P, Dumas P. A crystallographic study of the binding of 13 metal ions to two related RNA duplexes. *Nucleic Acids Res* 2003; 31:2671-82; PMID:12736317; <http://dx.doi.org/10.1093/nar/gkg350>.
83. Bernacchi S, Ennifar E, Tóth K, Walter P, Langowski J, Dumas P. Mechanism of hairpin-duplex conversion for the HIV-1 dimerization initiation site. *J Biol Chem* 2005; 280:40112-21; PMID:16169845; <http://dx.doi.org/10.1074/jbc.M503230200>.
84. Ennifar E, Bernacchi S, Wolff P, Dumas P. Influence of C-5 halogenation of uridines on hairpin versus duplex RNA folding. *RNA* 2007; 13:1445-52; PMID:17630326; <http://dx.doi.org/10.1261/rna.408507>.
85. Burnouf D, Ennifar E, Guedich S, Puffer B, Hoffmann G, Bec G, et al. kinITC: a new method for obtaining joint thermodynamic and kinetic data by isothermal titration calorimetry. *J Am Chem Soc* 2012; 134:559-65; PMID:22126339; <http://dx.doi.org/10.1021/ja209057d>.